

Generalized Non-Redundant Sparse Array Designs

Ammar Ahmed, *Student Member, IEEE*, and Yimin D. Zhang, *Fellow, IEEE*

Abstract—We present novel generalized non-redundant sparse array design strategies that achieve the highest possible number of degrees-of-freedom (DOFs) for direction-of-arrival (DOA) estimation. These array designs offer difference co-arrays that do not contain any lag redundancies except the unavoidable redundancies at lag zero. We first develop a co-array-based zero-redundancy design rule which serves as a baseline for constructing these non-redundant arrays, and a large-aperture naïve structured non-redundant sparse array is presented. We then develop a systematized design framework based on disjunctive programming to obtain non-redundant sparse array structures with a minimum array aperture, resulting in minimum hole arrays. The disjunctive programming framework is then extended to an equivalent mixed-integer linear programming problem. As a result, given the same number of physical sensors, the design framework provides a difference co-array with the maximum number of correlation lags and resolves more sources than existing sparse array structures. The non-redundant sparse array design is further generalized in two new directions, respectively achieving an arbitrary array aperture and reducing mutual coupling effects. Among the several new sparse array designs obtained from such generalizations, the hybrid non-redundant sparse array design simultaneously achieves the highest number of DOFs, meets a desired array aperture requirement, and reduces mutual coupling effects. Structured matrix completion methods are employed to interpolate the missing lags in the resulting difference co-arrays, thereby enabling high-resolution gridless DOA estimation with improved performance. Simulation results demonstrate the superiority of the generalized non-redundant sparse array design strategies over existing sparse array structures.

Index Terms—Sparse array, non-redundant array, difference co-array, direction-of-arrival estimation, matrix completion.

I. INTRODUCTION

DIRECTION-OF-ARRIVAL (DOA) estimation is a fundamental problem in sensor array signal processing with broad applications in radar, sonar, wireless communications, radio astronomy, and many other fields [1]. Based on the Nyquist sampling theorem, uniform linear array (ULA) has traditionally emerged as the most popular sensor array geometry for DOA estimation. ULA enjoys a simple regular array structure and well-analyzed signal processing techniques, but it generally resolves less sources than the number of sensors using the traditional methods assuming stationary sources. Therefore, significant efforts have been made to detect more sources than the number of sensors by employing sparse arrays in the context of difference co-arrays [2], [3]. Sparse arrays also reduce the undesirable mutual coupling effects as a result of larger inter-element spacing [4], [5].

The most well-known and fundamental sparse array structure is the minimum redundancy array (MRA) that achieves the maximum number of consecutive lags in the yielding difference co-array [3]. By constructing an augmented covariance matrix [6], MRA presents an optimal array geometry in the sense that it achieves the largest difference co-array aperture for a given number of sensors while producing the maximum number of continuous co-array lags. Another popular sparse array design is a non-redundant array with a minimum array aperture [7], also known as the minimum hole array (MHA) or Golomb array, that minimizes the number of holes in the difference co-array while achieving the maximum number of co-array lags. Traditionally, brute-force search has to be employed to design these arrays because there are no closed-form solutions for these array structures [3], [7], [8].

Recently, great attention has been paid to develop sparse array structures that can be systematically designed and analyzed. Two notable sparse arrays are the nested array [9] and the coprime array [10]. These array designs and their variants have been extensively studied, and their array structures and closed-form expressions for the achievable number of degrees-of-freedom (DOFs) are devised [11]–[15].

The nested array configuration uses two uniform linear sub-arrays [9] such that one of the sub-arrays has unit inter-element spacing whereas the other subarray has increased inter-element spacing. Nested array is known to provide a hole-free difference co-array. On the other hand, multiple level nested arrays [11] provide even more DOFs by allowing some holes in the resulting difference co-array. Two-dimensional extensions of nested arrays are given in [12], [13]. Super nested arrays [16] have the same physical aperture and the same hole-free coarray as the nested array; however, the number of sensor pairs with small separations is significantly reduced. Augmented nested arrays [14] employ the rearrangement of sensors by splitting the dense part of nested arrays resulting in an elongated difference co-array and reduced mutual coupling effects. Nested arrays and their variants, however, provide less DOFs compared to MRA or non-redundant arrays for the same number of physical sensors.

On the other hand, coprime array utilizes two uniform linear sub-arrays such that the number of elements in each sub-array is a coprime pair, and the inter-element spacing of each sub-array is proportional to the number of elements in the other sub-array [10]. The coprime array is generalized to configurations that achieve more consecutive and unique lags [15]. Compared to the nested array, the coprime array can further reduce mutual coupling effects due to its larger inter-element spacing, but offers a smaller number of DOFs. Similar to nested arrays, coprime arrays can also be arranged into multi-level designs [18], [19], although such designs do not generally yield a high number of unique lags. Efforts have

A. Ahmed was with the Department of Electrical and Computer Engineering, Temple University, Philadelphia, PA 19122. He is currently with Aptiv, Agoura Hills, CA 91301. (email: ammar.ahmed@aptiv.com)

Y. D. Zhang is with the Department of Electrical and Computer Engineering, Temple University, Philadelphia, PA 19122. (email: ydzhang@temple.edu)

been made to further improve the DOFs of the coprime array by minimizing the cross-subarray redundancies [20], but the achieved DOFs are still restricted due to the presence of self-redundancies of the uniform subarrays.

Design of non-redundant arrays has been a topic with great interest due to their ability to provide the highest number of DOFs [7], [8]. Non-redundant arrays generally yield holes in the rendered difference co-array and thus become difficult to exploit all co-array lags for subspace-based DOA estimation methods which requires the lags to be consecutive. On the other hand, compressive sensing-based DOA estimation methods can effectively use all the co-array lags [21]–[23]. In addition, exploiting Toeplitz structure-based covariance matrix interpolation strategies [24]–[27] can further provide higher estimation accuracy.

Optimal non-redundant array design through brute-force search for all the possible array configurations results in the minimum array aperture and maximum co-array lags [7], [8]. Side information can be employed to simplify the search operation. For example, [7] exploits the information that non-redundant arrays have a larger aperture than the MRA and that the sum of inter-element spacings in an array should be equal to the array aperture, whereas [8] assumes that there should be a pair of sensors with half-wavelength inter-element spacing at either edge of a non-redundant sparse array. Such side information is exploited to aid the design process and reduce the search space of the brute-force search [7], [8]. While brute-force search is time-consuming and infeasible for the design of large-size arrays, optimized design of non-redundant arrays with minimum aperture in the context of optimization is a challenging problem due to the integer variables involved in the design process.

Disjunctive programming [28]–[31] is an approach to model optimization problems that involve discrete and continuous variables, and exploits the inherent logic structure of the problems resulting in reduced combinatorics. In order to model discrete choices, disjunctive programming exploits relaxations by employing boolean variables and disjunctions. The problems based on generalized disjunctive programming (GDP) can contain a convex or non-convex objective function that needs to be optimized, boolean and continuous variables, algebraic constraints that need to be satisfied regardless of the discrete choices, disjunctions that represent the discrete choices, or logic propositions that contain the logic relationships between the boolean variables (for details, see [28]). Disjunctive linear programs can be converted to their integer counterparts by employing mixed-integer linear programming [32], [33]. MILP deals with the problems in which some of the variables are constrained to be integers while other variables are continuous. In this paper, we attack the non-redundant array design problem by exploiting GDP and MILP frameworks, which result in effective numerical optimizations.

The design of non-redundant arrays historically remained limited to MHA. Several efforts have been made in the past to design MHA using numerical search operations [7], [8], [34]. The formulations presented in this paper provide flexibility to add constraints based on aperture, inter-sensor spacing, and mutual coupling. Thus, in addition to effectively design

MHA structures, the proposed optimization frameworks also enable us to develop and optimize novel generalized non-redundant sparse array structures that account for several practical requirements. Two important issues are specially considered, namely, exploitation of an arbitrary array aperture and effective reduction of mutual coupling effects. In particular, the hybrid sparse array architecture offers both attractive features, i.e., support the specification of desirable array apertures and achieve reduced mutual coupling effects. Such new classes of generalized non-redundant sparse arrays open new possibilities for novel sparse arrays with many practical applications.

The main contributions of this paper are summarized as:

- Based on the co-array properties, we present a zero-redundancy rule for non-redundant sparse array design. Under this rule, we first develop a structured non-redundant sparse array, termed as naïve non-redundant array (NNRA), which guarantees the highest possible number of DOFs with a simple strategy. This simple design avoids redundancies by adding a new sensor with an inter-element spacing that is greater than the existing array aperture.
- By exploiting the non-redundant design rule, we develop a systematized framework based on disjunctive programming to design non-redundant sparse arrays with a minimum aperture, i.e., MHA. The disjunctive programming framework is effectively solved using two MILP approaches. Contrary to the classical approaches for designing non-redundant arrays, the proposed approach exploits optimization problems that fall in the category of GDP and MILP approaches, and provide flexibility by employing constraints based on the properties of their co-arrays.
- Non-redundant sparse array designs are generalized and three new types of structures are developed. The first type of non-redundant sparse arrays enables the use of any desired array aperture. The second type of non-redundant arrays results in reduced mutual coupling effects. The third type is a hybrid non-redundant sparse array which combines both above features, i.e., avoids the mutual coupling effects while enjoying the desired array aperture.
- We exploit compressive sensing-based strategy to estimate the DOA of incoming signals. In addition, we enable gridless DOA estimation using the subspace-based MUSIC [35] and ESPRIT [36] algorithms by employing the structured matrix completion which interpolates the holes in the resulting covariance matrix by exploiting its Toeplitz and Hermitian structure.

The rest of the paper is organized as follows. Signal models and necessary preliminaries are introduced in Section II. In Section III, we present the zero-redundancy design rule and propose the simple NNRA which achieves the highest DOFs with a large array aperture. Section IV proposes a systematic framework to design MHA which is an optimized non-redundant sparse array with the minimum aperture. The optimization problems are presented in the form of disjunctive as well as MILP approaches. In Section V, we generalize the non-redundant array design strategy and present three

new types of non-redundant arrays which achieve desired features of using flexible array apertures and reducing mutual coupling effects. Furthermore, we use an array interpolation strategy in Section VI to fill the holes in the proposed non-redundant array designs. Numerical results are provided in Section VII to demonstrate the superiority of the proposed array designs compared to popular sparse array structures. Finally, conclusions are drawn in Section VIII.

Notations: We use lower-case (upper-case) bold characters to denote vectors (matrices). In particular, \mathbf{I}_N denotes the $N \times N$ identity matrix, whereas $\mathbf{1}_N$ and $\mathbf{0}_N$ respectively denote the N -element column vectors of all ones and all zeros. Similarly, $\mathbf{O}_{M,N}$ denotes a null matrix of size $M \times N$. $(\cdot)^T$ and $(\cdot)^H$ respectively represent the transpose and conjugate transpose of a matrix or vector, $\text{vec}(\cdot)$ is the vectorization operator that turns a matrix into a vector by stacking all columns on top of the another, $\text{diag}(\mathbf{x})$ denotes a diagonal matrix that uses the elements of vector \mathbf{x} as its diagonal elements, and $\mathbf{v} \odot \mathbf{w}$ is the elementwise product between two vectors \mathbf{v} and \mathbf{w} . Notation $\text{tr}(\cdot)$ represents the trace of a matrix, whereas the expression $\mathbf{X} \succeq 0$ represents a non-negative semidefinite matrix \mathbf{X} . The inequality equation $\mathbf{A} \neq \mathbf{B}$ illustrates that each element in matrix \mathbf{A} is not equal to the corresponding element in matrix \mathbf{B} where matrices \mathbf{A} and \mathbf{B} have the same size. For matrix \mathbf{A} , $\mathbf{A}^{[l]}$ is the matrix obtained by deleting the l th row of matrix \mathbf{A} , the row vector $\mathbf{a}^{(l)}$ denotes the l th row of \mathbf{A} , whereas $\mathbf{A}_{(i,j)}$ denotes the element on the i th row and the j th column of \mathbf{A} . In addition, $\|\cdot\|_F$, $\|\cdot\|_0$, and $\|\cdot\|_1$ denote the Frobenius norm, l_0 -norm, and l_1 -norm, respectively. Moreover, $\mathbb{E}[\cdot]$ is the statistical expectation operator, and \otimes denotes the Kronecker product.

II. PRELIMINARIES

A. Signal Model

Consider an N -element sparse sensor array whose sensor positions are given by $p_1 \cdot \lambda/2, \dots, p_N \cdot \lambda/2$, where λ is the signal wavelength and p_1, \dots, p_N are the non-negative integer numbers. The first sensor position is considered as the reference such that $p_1 = 0$. Without loss of generality, the sensor positions are assumed to be in the ascending order, i.e., $p_n < p_{n+1}$ for $n = 1, \dots, N-1$.

Assume that Q uncorrelated narrowband far-field signals impinge on the sparse array from distinct angles $\{\theta_1, \dots, \theta_Q\}$ with respective powers $\{\sigma_1^2, \sigma_2^2, \dots, \sigma_Q^2\}$. The baseband data vector $\mathbf{x}(t)$ received at the sensor array at time instant t can be modeled as:

$$\mathbf{x}(t) = \sum_{q=1}^Q s_q(t) \mathbf{a}(\theta_q) + \mathbf{n}(t) = \mathbf{A} \mathbf{s}(t) + \mathbf{n}(t), \quad (1)$$

where $s_q(t)$ denotes the baseband waveform of the q th signal and $\mathbf{s}(t) = [s_1(t), \dots, s_Q(t)]^T$ denotes the signal vector. The elements of the noise vector $\mathbf{n}(t) \sim \mathcal{CN}(\mathbf{0}_N, \bar{\sigma}_n^2 \mathbf{I}_N)$ are assumed to be independent and identically distributed (i.i.d.) complex white Gaussian random processes and are assumed to be uncorrelated from the impinging sources. Here, $\bar{\sigma}_n^2$ represents the noise variance. The matrix $\mathbf{A} = [\mathbf{a}(\theta_1),$

$\dots, \mathbf{a}(\theta_Q)]$ represents the array manifold with $\mathbf{a}(\theta_q)$ denoting the array steering vector corresponding to angle θ_q given as:

$$\mathbf{a}(\theta_q) = [1, e^{j\pi p_2 \sin(\theta_q)}, \dots, e^{j\pi p_N \sin(\theta_q)}]^T, \quad (2)$$

where $j = \sqrt{-1}$. The covariance matrix of the received data vector $\mathbf{x}(t)$ can be obtained as:

$$\begin{aligned} \mathbf{R}_x &= \mathbb{E}[\mathbf{x}(t) \mathbf{x}^H(t)] = \mathbf{A} \mathbf{R}_s \mathbf{A}^H + \bar{\sigma}_n^2 \mathbf{I}_N \\ &= \sum_{q=1}^Q \sigma_q^2 \mathbf{a}(\theta_q) \mathbf{a}^H(\theta_q) + \bar{\sigma}_n^2 \mathbf{I}_N, \end{aligned} \quad (3)$$

where $\mathbf{R}_s = \mathbb{E}[\mathbf{s}(t) \mathbf{s}^H(t)] = \text{diag}([\sigma_1^2, \sigma_2^2, \dots, \sigma_Q^2])$ is the source covariance matrix. In practice, the covariance matrix \mathbf{R}_x is estimated from the sample average of T samples as:

$$\hat{\mathbf{R}}_x = \frac{1}{T} \sum_{t=0}^{T-1} \mathbf{x}(t) \mathbf{x}^H(t). \quad (4)$$

B. Difference Co-array

Vectorizing \mathbf{R}_x yields

$$\mathbf{z} = \text{vec}(\mathbf{R}_x) = \tilde{\mathbf{A}} \mathbf{b} + \bar{\sigma}_n^2 \tilde{\mathbf{i}}, \quad (5)$$

where $\tilde{\mathbf{A}} = [\tilde{\mathbf{a}}(\theta_1), \dots, \tilde{\mathbf{a}}(\theta_Q)]$, $\tilde{\mathbf{a}}(\theta_q) = \mathbf{a}^*(\theta_q) \otimes \mathbf{a}(\theta_q)$, $\mathbf{b} = [\sigma_1^2, \sigma_2^2, \dots, \sigma_Q^2]^T$, and $\tilde{\mathbf{i}} = \text{vec}(\mathbf{I}_N)$. Comparing Eqs. (1) and (5), the new vector \mathbf{z} can be viewed as a single-snapshot received data vector corresponding to a single-snapshot source signal vector \mathbf{b} , whereas $\bar{\sigma}_n^2 \tilde{\mathbf{i}}$ becomes a deterministic term. The distinct columns of $\tilde{\mathbf{A}}$ act as the virtual array manifold of an extended array aperture. The positions of this virtual array are termed as the difference co-array of the original array and can be represented as set \mathbb{D} . Denote $\mathbb{P} = \{p_1, \dots, p_N\}$ as an integer set representing the sensor positions on half-wavelength grid. The difference co-array \mathbb{D} containing difference lags can be expressed as [15]:

$$\mathbb{D} = \mathbb{P} \ominus \mathbb{P} = \bigcup_{\forall p_l, p_k \in \mathbb{P}} \{p_l - p_k\}, \quad (6)$$

where \ominus represents the difference co-array operator.

The number of DOFs of a sparse array configuration is determined by $(\eta + 1)/2$ where η is the achieved number of unique correlation lags of the difference co-array. Therefore, η is equal to the number of elements in the set represented by Eq. (6). It is highly desirable to design a sensor array which provides a high number of co-array lags since it is directly associated with the number of sources that can be resolved [15].

C. Mutual Coupling

The signal model in Eq. (1) does not contain the artifacts introduced due to the mutual coupling among different sensors. In practice, mutual coupling among closely-spaced sensors cannot be neglected. A simplistic model incorporating these mutual coupling effects can be expressed as [5]:

$$\mathbf{x}(t) = \mathbf{C} \mathbf{A} \mathbf{s}(t) + \mathbf{n}(t), \quad (7)$$

where the element on the i th row and the j th column of \mathbf{C} is given by:

$$\mathbf{C}_{(i,j)} = \begin{cases} c_{|p_i - p_j|}, & |p_i - p_j| \leq C, \\ 0, & \text{otherwise,} \end{cases} \quad (8)$$

where $i, j = 1, \dots, N$. This model assumes that the mutual coupling effects are negligible for the sensors that are more than $C\lambda/2$ apart. The coefficients c_i are the coupling coefficients satisfying $c_0 = 1 > |c_1| > |c_2| > \dots > |c_C|$. It is assumed that the magnitudes of mutual coupling coefficients are inversely proportional to the sensor separations. It is well-known that the co-array weight functions at small separations play pivotal role in introducing mutual coupling artifacts. In particular, the first two co-array weights have the highest impact on mutual coupling of an array [5], [16].

III. NON-REDUNDANT SPARSE ARRAYS

Non-redundant arrays enjoy highest number of DOFs by achieving the maximum possible number of unique lags in the resulting difference co-array. All the non-zero co-array lags of a non-redundant sparse array are unique. Note that N sensors yield N entries of lag-0 self-lags which cannot be avoided. Therefore, for a non-redundant array consisting of N sensors, we have a total of N^2 co-array lags among which N lags are located at position 0. This implies that a non-redundant array of N sensors achieves $N^2 - N + 1$ unique co-array lags.

In this section, we describe the zero-redundancy condition which is necessary for the development of non-redundant sparse arrays. Subsequently, we will first present an NNRA design which satisfies the zero-redundancy condition. However, the resulting NNRA configurations have large inter-element spacing which can give rise to high sidelobe level for DOA estimates. In order to counter this disadvantage and design non-redundant sparse arrays with minimum aperture, we then develop a systematic design framework in the next section by employing the disjunctive and MILP methods. These results are then generalized to develop three new types of non-redundant arrays which enjoy the desired features of using flexible array aperture and reducing mutual coupling effects.

Define position vector $\mathbf{p} = [p_1, p_2, \dots, p_N]^T$. Our objective is to determine the optimal \mathbf{p} for the sparse array such that the corresponding difference co-array contains the maximum number of unique lags for any given number of sensors. This can only be possible if the difference co-array of the designed sensor array contains no lag redundancies except at lag 0.

A. Zero-Redundancy Design Rule

From Eq. (6), we know that redundancies will be present in the co-array if different pairs of sensor positions result in a same co-array lag. Ignoring the redundancies at lag 0, all co-array lags are unique if the co-array lag generated from a pair of sensor elements is not equal to the co-array lag generated by another pair of sensor elements, i.e.,

$$p_i - p_j \neq p_k - p_l, \quad \begin{matrix} i, j, k, l = 1, \dots, N, \\ i \neq j, k \neq l, j \neq l. \end{matrix} \quad (9)$$

The conditions $i \neq j$ and $k \neq l$ ensure that the co-array lags positioned at 0 are ignored, whereas $j \neq l$ ensures that only

different pairs of sensors are considered. Incorporating the fact that sensor positions are sorted in an ascending order in Eq. (9), we obtain the following zero-redundancy design rule [34]:

$$p_i + 1 \leq p_{i+1} \text{ and } p_j - p_k \neq p_l - p_m, \quad j \neq k, l \neq m, k \neq m, \quad (10)$$

where $i = 1, \dots, N-1$ and $j, k, l, m = 1, \dots, N$. This condition ensures the sparse array to be a non-redundant one.

B. A Naïve Non-redundant Array

Non-redundant arrays following the design rule in Eq. (10) are not unique. That is, for a given number of physical sensors, we can design multiple non-redundant arrays which all result in the same maximum number of unique lags. A naïve approach for such an array design can be obtained by choosing the inter-element spacing between the $(n-1)$ th and n th sensors to be greater than the array aperture till the $(n-1)$ th sensor, i.e., $p_n - p_{n-1} > p_{n-1}$. The sensor positions for such a naïve design can be found as:

$$p_n \geq 2p_{n-1} + 1, \quad n = 2, \dots, N. \quad (11)$$

NNRA with the smallest aperture leads to the optimally nested array (ONA) [9]. The sensor locations for this case can be given by $p_n = 2^{n-1} - 1$ for $n = 1, 2, \dots, N$, resulting in the array aperture of $2^{N-1} - 1$. Such a large aperture renders a high level of sensor sparsity and gives rise to inherent high sidelobe levels for the DOA estimates. To overcome this problem, we consider optimized non-redundant array designs in the following sections.

IV. OPTIMIZED NON-REDUNDANT SPARSE ARRAY DESIGN

In this section, we optimize the non-redundant sparse array design such that the resulting sparse array provides the maximum number of unique lags for the smallest possible array aperture, i.e. an MHA is formed. In order to design such an array, we formulate a comprehensive design framework to implement the zero-redundancy design rule using disjunctive programming [28]–[31]. This framework is then reformulated as MILP optimization problems [32], [33] to enable effective solutions. In the next section, we generalize this design and present three special cases of the generalized non-redundant sparse arrays that are specifically designed to achieve a desired array aperture, reduce the mutual coupling effects, or both.

Under the design rule in Eq. (10), we formulate the following optimization problem to ensure a minimum array aperture [34]:

$$\begin{aligned} & \min_{p_n \in \mathbb{Z}^+, \forall n} p_N \\ & \text{subject to} \quad p_i + 1 \leq p_{i+1}, \quad i = 1, \dots, N-1, \\ & \quad \quad \quad p_i - p_j \neq p_k - p_l, \quad \begin{matrix} i \neq j, k \neq l, j \neq l, \\ i, j, k, l = 1, \dots, N. \end{matrix} \end{aligned} \quad (12)$$

Here, \mathbb{Z}^+ represents the set of all non-negative integers. Since the difference co-array is symmetric in nature, i.e., the negative and positive lag positions are symmetric around the lag 0, the above optimization problem can be considered only for the positive side of the co-array. This will provide the same resulting co-array while reducing the search space of the

optimization problem. Therefore, we can employ $i > j$ and $k > l$ so that the lags $p_i - p_j$ and $p_k - p_l$ are guaranteed to be positive [34], i.e.,

$$\begin{aligned} & \min_{p_n \in \mathbb{Z}^+, \forall n} p_N \\ & \text{subject to} \quad p_i + 1 \leq p_{i+1}, \quad i = 1, \dots, N-1, \\ & \quad \quad \quad p_i - p_j \neq p_k - p_l, \quad i > j, k > l, j \neq l, \\ & \quad \quad \quad i, j, k, l = 1, \dots, N. \end{aligned} \quad (13)$$

In the following subsection, we employ a systematic strategy to solve this optimization problem by employing disjunctive programming which is subsequently expanded to two different MILP optimization problems.

A. Disjunctive Programming Framework

Consider an $(N-1) \times N$ upper bidiagonal matrix \mathbf{S} such that all main diagonal elements are equal to -1 , all upper diagonal elements are equal to 1 , whereas the remaining elements are zero. This implies that $\mathbf{S}_{(i,i)} = -1$ and $\mathbf{S}_{(i,i+1)} = 1$ for $i = 1, \dots, N-1$. We ensure the uniqueness of sensor positions, i.e., $p_N > p_{N-1} > \dots > p_1$, by introducing the following element-wise inequality:

$$\mathbf{S}\mathbf{p} \geq \mathbf{1}_{N-1}. \quad (14)$$

Now, we formulate the positive-lag uniqueness condition in optimization problem (13) in the form of a disjunction. For this purpose, we first construct a combination matrix \mathbf{J} which translates the sensor positions \mathbf{p} into their respective positive co-array. The matrix \mathbf{J} , containing $U = N(N-1)/2$ rows and N columns, takes the following form:

$$\mathbf{J} = [\mathbf{J}_1^T, \mathbf{J}_2^T, \dots, \mathbf{J}_{N-1}^T]^T, \quad (15)$$

where

$$\mathbf{J}_i = [\mathbf{0}_{N-i, i-1}, -\mathbf{1}_{N-i}, \mathbf{I}_{N-i}], \quad i = 1, \dots, N-1. \quad (16)$$

For instance, when $N = 4$, matrix \mathbf{J} is given by:

$$\mathbf{J} = \begin{bmatrix} -1 & 1 & 0 & 0 \\ -1 & 0 & 1 & 0 \\ -1 & 0 & 0 & 1 \\ 0 & -1 & 1 & 0 \\ 0 & -1 & 0 & 1 \\ 0 & 0 & -1 & 1 \end{bmatrix}.$$

The vector $\mathbf{J}\mathbf{p}$ will result in all the possible positive co-array lags which an N -element sensor array \mathbb{P} can provide. The elements in $\mathbf{J}\mathbf{p}$ are generally not in an ascending or descending order. As we only examine the positive co-array lags, when all those positive lags in $\mathbf{J}\mathbf{p}$ are unique, the corresponding negative co-array lags in $-\mathbf{J}\mathbf{p}$ are also unique.

The condition that all elements of vector $\mathbf{J}\mathbf{p}$ are unique can be described as the following element-wise inequality:

$$\mathbf{1}_{U-1} \mathbf{j}^{(u)} \mathbf{p} \neq \mathbf{J}^{[u]} \mathbf{p}, \quad u = 1, \dots, U. \quad (17)$$

Define $L \times N$ matrices

$$\mathbf{J}_A = \begin{bmatrix} \mathbf{1}_{U-1} \mathbf{j}^{(1)} \\ \vdots \\ \mathbf{1}_{U-1} \mathbf{j}^{(U)} \end{bmatrix} \quad \text{and} \quad \mathbf{J}_B = \begin{bmatrix} \mathbf{J}^{[1]} \\ \vdots \\ \mathbf{J}^{[U]} \end{bmatrix},$$

where $L = U(U-1)$. Then, Eq. (17) can be expressed in the following compact form:

$$\mathbf{J}_A \mathbf{p} \neq \mathbf{J}_B \mathbf{p}. \quad (18)$$

Using Eqs. (14) and (18), optimization problem (13) can be expressed as the following disjunctive programming problem:

$$\begin{aligned} & \min_{p_n \in \mathbb{Z}^+, \forall n} p_N \\ & \text{subject to} \quad \mathbf{S}\mathbf{p} \geq \mathbf{1}_{N-1}, \\ & \quad \quad \quad \Omega(\mathbf{j}_A^{(l)} \mathbf{p} \neq \mathbf{j}_B^{(l)} \mathbf{p}) = \text{True}, \quad l = 1, \dots, L. \end{aligned} \quad (19)$$

Here, $\Omega(\cdot)$ is a logical operator which returns a ‘True’ value if the element $\mathbf{j}_A^{(l)} \mathbf{p}$ is not equal to the element $\mathbf{j}_B^{(l)} \mathbf{p}$. Optimization problem (19) is one of disjunctive programming-based representations which satisfy the zero-redundancy design rule depicted in Eq. (10). Since \mathbf{p} is a vector of integers, the logic proportion will be true only if $\mathbf{j}_A^{(l)} \mathbf{p} + 1 \leq \mathbf{j}_B^{(l)} \mathbf{p}$ or $\mathbf{j}_A^{(l)} \mathbf{p} \geq \mathbf{j}_B^{(l)} \mathbf{p} + 1$.

Another disjunctive optimization problem which also yields a non-redundant array with a minimum aperture is formulated in the following form:

$$\begin{aligned} & \min_{p_n \in \mathbb{Z}^+, \forall n, z_l \in \{0,1\}, \forall l} p_N \\ & \text{subject to} \quad \mathbf{S}\mathbf{p} \geq \mathbf{1}_{N-1}, \\ & \quad \quad \quad \left[\mathbf{j}_A^{(l)} \mathbf{p} + 1 \leq \mathbf{j}_B^{(l)} \mathbf{p} \right] \vee \left[\mathbf{j}_A^{(l)} \mathbf{p} \geq \mathbf{j}_B^{(l)} \mathbf{p} + 1 \right], \end{aligned} \quad (20)$$

where \vee represents a disjunction or logical OR operator which is ensured for each $l \in \{1, \dots, L\}$. The inequality on the left hand side of \vee is satisfied if $z_l = 1$, whereas the inequality on the right hand side of \vee is satisfied if $z_l = 0$. For instance, if all the elements in $\mathbf{z} = [z_1, z_2, \dots, z_L]^T$ are unity, i.e., $\mathbf{z} = \mathbf{1}_L$, the element-wise inequality $\mathbf{J}_A \mathbf{p} + \mathbf{1}_L \leq \mathbf{J}_B \mathbf{p}$ will be satisfied. It not only ensures the minimum array aperture by minimizing p_N , but also ensures that the element-wise inequality $\mathbf{J}_A \mathbf{p} \neq \mathbf{J}_B \mathbf{p}$ is satisfied, thereby resulting in a non-redundant sparse array. Optimization problem (20) can also be simplified as:

$$\begin{aligned} & \min_{p_n \in \mathbb{Z}^+, \forall n, z_l \in \{0,1\}, \forall l} p_N \\ & \text{subject to} \quad \mathbf{S}\mathbf{p} \geq \mathbf{1}_{N-1}, \\ & \quad \quad \quad \left[\mathbf{k}^{(l)} \mathbf{p} \leq -1 \right] \vee \left[\mathbf{k}^{(l)} \mathbf{p} \geq 1 \right], \quad l = 1, \dots, L, \end{aligned} \quad (21)$$

where $\mathbf{k}^{(l)} = \mathbf{j}_A^{(l)} - \mathbf{j}_B^{(l)}$. Alternatively, the condition $\Omega(\mathbf{j}_A^{(l)} \mathbf{p} \neq \mathbf{j}_B^{(l)} \mathbf{p})$ can be expressed as $\Omega(\mathbf{k}^{(l)} \mathbf{p} \neq 0)$ in problem (19).

The optimization problems (19), (20) and (21) fall in the category of GDP [29]. There exist several solvers to solve GDP problems [29]–[31]. However, many solvers only allow continuous variables within the objective function, the disjunction, and boolean variables within $\Omega(\cdot)$. Because the optimization problems (19), (20), and (21) involve integer variable \mathbf{p} , some GDP solvers may not be directly applicable. In order to solve these optimization problems with a high flexibility, we convert disjunctive programming problems into MILP counterparts in the next section which can be handled by popular MILP solvers [32], [33].

B. Mixed-Integer Linear Programming Framework

GDP problems can be solved by exploiting MILP. As integer variables are involved in solving them, they are more computationally expensive than linear programming problems. A good way to approach an MILP problem is to obtain an initial guess by exploiting the relaxed version of the problem. This initial solution is then employed by advanced branch-and-bound or branch-and-cut algorithms to obtain the optimal solution.

In this subsection, we present two ways to convert optimization problems (19) and (21) into their MILP counterpart that can also be relaxed to obtain suboptimal solutions. The first method, called Big-M formulation, employs an additional variable M which helps convert the logical disjunctions into constraints. The second method, named Convex-Hull formulation, exploits the same principle but uses more variables than the big-M method. If the binary variables of these problems are relaxed to span the continuous region between 0 and 1, their respective solutions can be used as an initial guess [28]–[30]. While Convex-Hull and Big-M formulations result in problems that represent identical solution spaces, their relaxed problems are not identical. The solution space resulting from the Big-M formulation is larger than the minimum solution space for the Convex-Hull formulation. This results in fewer iterations required to solve the relaxed GDP problems formulated using Convex-Hull. Despite this, the Big-M formulation is simpler and requires less variables. Due to this reason, Big-M formulation tends to converge faster for the branch-and-bound and branch-and-cut-based integer programming solvers given that its relaxed solution space is the same [28], [29].

1) *Big-M Formulation*: In this type of formulation, we define a sufficiently large constant M . Then, each inequality requirement can be reformulated such that, if it is not being used, it becomes null and void. This implies that we modify the inequalities on both sides of disjunction in optimization problem (21) such that the unused inequalities are ignored. The resulting optimization problem takes the following form:

$$\begin{aligned} & \min_{p_n \in \mathbb{Z}^+, \forall n, z_l \in \{0,1\}, \forall l} p_N \\ & \text{subject to} \quad \mathbf{S}\mathbf{p} \geq \mathbf{1}_{N-1}, \\ & \quad 1 - Mz_l \leq \mathbf{k}^{(l)}\mathbf{p}, \quad l = 1, \dots, L, \\ & \quad \mathbf{k}^{(l)}\mathbf{p} \leq -1 + M(1 - z_l), \quad l = 1, \dots, L. \end{aligned} \quad (22)$$

Note that if $z_l = 0$, $1 \leq \mathbf{k}^{(l)}\mathbf{p}$ is satisfied, whereas $\mathbf{k}^{(l)}\mathbf{p} \leq -1$ is satisfied for $z_l = 1$. Moreover, the conditions $\mathbf{k}^{(l)}\mathbf{p} \leq -1 + M$ and $1 - M \leq \mathbf{k}^{(l)}\mathbf{p}$ are redundant due to a very large value of M which is intelligently selected.

2) *Convex-Hull Formulation*: Another form of the MILP optimization problem for extracting non-redundant arrays can be given as:

$$\begin{aligned} & \min_{p_n \in \mathbb{Z}^+, \forall n, z_l \in \{0,1\}, \forall l} p_N \\ & \text{subject to} \quad \mathbf{S}\mathbf{p} \geq \mathbf{1}_{N-1}, \\ & \quad -Mz_l \leq \mathbf{k}^{(l)}\mathbf{p}_1 \leq -z_l, \quad l = 1, \dots, L, \\ & \quad 1 - z_l \leq \mathbf{k}^{(l)}\mathbf{p}_2 \leq M(1 - z_l), \quad l = 1, \dots, L, \\ & \quad \mathbf{p}_1 + \mathbf{p}_2 = \mathbf{p}. \end{aligned} \quad (23)$$

Here, \mathbf{p}_1 and \mathbf{p}_2 are intermediary variables which add to make the variable of interest \mathbf{p} . Note that if $z_l = 0$, we have $0 \leq \mathbf{k}^{(l)}\mathbf{p}_1 \leq 0$ which results in the elements of \mathbf{p}_1 corresponding to the non-zero elements in $\mathbf{k}^{(l)}$ equal to zero. Similarly, the entries of \mathbf{p}_2 for $z_l = 1$ corresponding to $0 \leq \mathbf{k}^{(l)}\mathbf{p}_2 \leq 0$ will also be equal to zero. The optimization problem (23) ensures that $\mathbf{k}^{(l)}\mathbf{p}$ is either positive or negative. Due to the presence of intermediary variables, the optimization problem (23) involves more variables than the optimization problem (22).

In optimization problems (22) and (23), the value of M should be ideally equal to the aperture of the array. Big values of M will lead to a very large search space resulting in increased computational burden. On the other hand, the optimization problems will become infeasible if the value of M is smaller than the array aperture. For an N -element sparse array, the array aperture A is given by [8]:

$$A = p_N = \frac{N(N-1)}{2} + H - R, \quad (24)$$

where R is the number of redundancies and H is the number of holes in the non-negative difference co-array.

The lower bound of the number of redundancies and holes in the difference co-array of a sparse array is further expressed as [8]:

$$R(6\pi + 4) + H(6\pi - 4) \geq 2N^2 - N(3\pi + 2) + 3\pi + 2. \quad (25)$$

Since $R = 0$ for non-redundant arrays, we obtain from Eq. (25):

$$H \geq \frac{N^2}{3\pi - 2} - \frac{(N-1)(3\pi + 2)}{2(3\pi - 2)}. \quad (26)$$

This lower bound of the number of holes increases to $N^2/(3\pi - 2)$ when N is large. Subsequently, the ratio between N^2 and the aperture is given by:

$$\frac{N^2}{A} = \frac{N^2}{\frac{N}{2}(N-1) + H}. \quad (27)$$

Substituting Eq. (26) into Eq. (27), we obtain:

$$A \geq \frac{N}{2}(N-1) + \frac{N^2}{3\pi - 2} - \frac{(N-1)(3\pi + 2)}{2(3\pi - 2)}, \quad (28)$$

which acts as the lower bound on M for optimization problems (22) and (23). For very large arrays, $\frac{N^2}{A} \rightarrow 1$ [37]. Therefore, the value of M is upper bounded by N^2 . Both optimization problems (22) and (23) can be exploited directly to extract the non-redundant arrays and can be solved using popular MILP solvers like Gurobi [32] and MOSEK [33]. Such modern solvers exploit advanced branch-and-cut algorithms along with the pre-solving capabilities. Unlike the brute-force search, MILP solvers keep the track of bounds on the minimum within which the solution of MILP optimization problem exists. This enables them to prune the search space and eliminate the candidate solutions that do not belong to the optimal solution set. Conventionally, these algorithms have been found to perform far better than the brute-force search [32], [33]. However, the exact computational cost varies with different problems and, in the worst-case scenario, the computational cost can be the same as brute-force search. Some MILP solvers also allow to terminate the search procedure before an exact

solution is achieved. In this scenario, we can constrain the complexity in polynomial time; however, the solution will be approximate.

Several other candidate constraints can also be added in the optimization problems (22) and (23) to aid the advanced cutting plane methods used by the MILP solvers. For example, the sum of all the inter-element spacings of an array is equal to its aperture. Moreover, we know from Eq. (24) that the aperture of the non-redundant array always is greater than $\frac{N(N-1)}{2}$. Such example constraints can be expressed as:

$$p_N = \mathbf{1}_{N-1}^T \mathbf{S}\mathbf{p}, \quad p_N \geq \frac{N(N-1)}{2}. \quad (29)$$

Such constraints can be readily added in our proposed optimization problems (22) and (23) to boost the search operation as they can reduce the search space of these MILP optimization problems.

V. GENERALIZED NON-REDUNDANT ARRAY DESIGN

In this section, we generalize the concept of non-redundant sparse array design to further enjoy important features, such as using a flexible sparse array aperture and reducing the undesired mutual coupling effects. This is considered by proposing three cases of new non-redundant sparse arrays. First, we develop non-redundant sparse arrays having a desired array aperture. Second, we present non-redundant array designs which effectively reduce the mutual coupling effects compared to the other array structures. Finally, we present a hybrid non-redundant array which simultaneously enjoys both features of a desired array aperture and mutual coupling reduction.

A. Non-redundant Arrays with Desired Array Aperture

Let \bar{M} be the array aperture of a non-redundant array with a minimum aperture. If \bar{A} is the desired array aperture for the non-redundant array such that $\bar{A} \geq \bar{M}$, we can reformulate optimization problem (19) as:

$$\begin{aligned} & \max_{p_n \in \mathbb{Z}^+, \forall n} && p_N \\ & \text{subject to} && p_N \leq \bar{A}, \\ & && \mathbf{S}\mathbf{p} \geq \mathbf{1}_{N-1}, \\ & && \Omega(\mathbf{j}_A^{(l)} \mathbf{p} \neq \mathbf{j}_B^{(l)} \mathbf{p}) = \text{True}, \quad l = 1, \dots, L. \end{aligned} \quad (30)$$

The above optimization problem provides a non-redundant array with the specified aperture \bar{A} . Alternatively, we can reformulate the disjunctive optimization problem (20) for non-redundant array design with a desired array aperture as:

$$\begin{aligned} & \max_{p_n \in \mathbb{Z}^+, \forall n, z_l \in \{0,1\}, \forall l} && p_N \\ & \text{subject to} && p_N \leq \bar{A}, \\ & && \mathbf{S}\mathbf{p} \geq \mathbf{1}_{N-1}, \\ & && \left[\mathbf{J}_A \mathbf{p} \geq \mathbf{J}_B \mathbf{p} + \mathbf{1} \right] \vee \left[\mathbf{J}_A^{(l)} \mathbf{p} + \mathbf{1} \leq \mathbf{J}_B^{(l)} \mathbf{p} \right]. \end{aligned} \quad (31)$$

The corresponding MILP optimization employing big-M formulation is obtained by substituting M by \bar{A} given as:

$$\begin{aligned} & \max_{p_n \in \mathbb{Z}^+, \forall n, z_l \in \{0,1\}, \forall l} && p_N \\ & \text{subject to} && p_N \leq \bar{A}, \\ & && \mathbf{S}\mathbf{p} \geq \mathbf{1}_{N-1}, \\ & && 1 - \bar{A}z_l \leq \mathbf{k}^{(l)} \mathbf{p}, \quad l = 1, \dots, L, \\ & && \mathbf{k}^{(l)} \mathbf{p} \leq -1 + \bar{A}(1 - z_l), \quad l = 1, \dots, L. \end{aligned} \quad (32)$$

Similarly, we can obtain the corresponding Convex-Hull formulation as:

$$\begin{aligned} & \max_{p_n \in \mathbb{Z}^+, \forall n, z_l \in \{0,1\}, \forall l} && p_N \\ & \text{subject to} && p_N \leq \bar{A}, \\ & && \mathbf{S}\mathbf{p} \geq \mathbf{1}_{N-1}, \\ & && -\bar{A}z_l \leq \mathbf{k}^{(l)} \mathbf{p}_1 \leq -z_l, \quad l = 1, \dots, L, \\ & && 1 - z_l \leq \mathbf{k}^{(l)} \mathbf{p}_2 \leq \bar{A}(1 - z_l), \quad l = 1, \dots, L, \\ & && \mathbf{p}_1 + \mathbf{p}_2 = \mathbf{p}. \end{aligned} \quad (33)$$

The MILP problems (32) and (33) can be used to extract non-redundant sparse arrays with a desired array aperture \bar{A} . Although inequality $p_N \leq \bar{A}$ is used in these optimization problems, we have confirmed via simulations for $M = 4, \dots, 10$ sensors, that such non-redundant arrays exist for all the possible array apertures within the range $\bar{M} \leq \bar{A} \leq M^2$.

B. Non-redundant Arrays with Reduced Mutual Coupling

In this subsection, we design non-redundant arrays with reduced mutual coupling effects. This is ensured by designing the non-redundant arrays such that the resulting co-array has L_m consecutive holes in the co-array at lag positions $1, \dots, L_m$, where L_m is a small positive integer. The motivation behind this array design is to avoid small co-array lag values as they most significantly contribute to the mutual coupling effects. In particular, co-array lag values of 1, 2 and 3 have a major impact on the mutual coupling of an array, with lag 1 showing the highest impact [4], [5], [16].

Our objective can be achieved in two ways. Since vector $\mathbf{S}\mathbf{p}$ contains all the inter-element spacings between consecutive sensors, we can replace the constraint $\mathbf{S}\mathbf{p} \geq \mathbf{1}_{N-1}$ in Eqs. (19) and (21) by $\mathbf{S}\mathbf{p} \geq (1 + L_m)\mathbf{1}_{N-1}$ so that lag positions $1, \dots, L_m$ are eliminated. Another approach is to utilize the fact that vector $\mathbf{J}\mathbf{p}$ provides all the positive co-array lags. Instead of using $\mathbf{S}\mathbf{p} \geq (1 + L_m)\mathbf{1}_{N-1}$, we can add a constraint $\mathbf{J}\mathbf{p} \geq (1 + L_m)\mathbf{1}_U$ in optimization problems (19) and (21).

The corresponding MILP optimization using big-M formulation is expressed as:

$$\begin{aligned} & \min_{p_n \in \mathbb{Z}^+, \forall n, z_l \in \{0,1\}, \forall l} && p_N \\ & \text{subject to} && \mathbf{S}\mathbf{p} \geq (1 + L_m)\mathbf{1}_{N-1}, \\ & && 1 - Mz_l \leq \mathbf{k}^{(l)} \mathbf{p}, \quad l = 1, \dots, L, \\ & && \mathbf{k}^{(l)} \mathbf{p} \leq -1 + M(1 - z_l), \quad l = 1, \dots, L. \end{aligned} \quad (34)$$

The Convex-Hull formulation takes the following form:

$$\begin{aligned}
& \min_{p_n \in \mathbb{Z}^+, \forall n, z_l \in \{0,1\}, \forall l} p_N \\
& \text{subject to} \quad \mathbf{Sp} \geq (1 + L_m)\mathbf{1}_{N-1}, \\
& \quad -Mz_l \leq \mathbf{k}^{(l)}\mathbf{p}_1 \leq -z_l, \quad l = 1, \dots, L, \\
& \quad 1 - z_l \leq \mathbf{k}^{(l)}\mathbf{p}_2 \leq M(1 - z_l), \quad l = 1, \dots, L, \\
& \quad \mathbf{p}_1 + \mathbf{p}_2 = \mathbf{p}.
\end{aligned} \tag{35}$$

Note that the new array will have a larger aperture than \bar{M} because the resulting co-array contains more holes. Specifically, the smallest inter-element spacing is increased from 1 to $L_m + 1$. For the pairs of sensors in the non-redundant array with minimum aperture which result in lags at positions $1, 2, \dots, L_m$, the corresponding inter-element spacing should be increased by at least $L_m, L_m - 1, \dots, 1$, respectively, which leads to additional holes in the resulting difference co-array. Therefore, if the non-redundant array with a minimum aperture had no co-array holes from lag 1 to lag L_m , the new non-redundant array with reduced mutual coupling will introduce at least the following number of holes in the co-array:

$$H_m = L_m + (L_m - 1) + \dots + 1 = \sum_{k=1}^{L_m} k = \frac{L_m(L_m + 1)}{2}. \tag{36}$$

The new lower bound on M for optimization problems (34) and (35) can be obtained from Eqs. (28) and (36) as:

$$A \geq H_m + \frac{N}{2}(N - 1) + \frac{N^2}{3\pi - 2} - \frac{(N - 1)(3\pi + 2)}{2(3\pi - 2)}. \tag{37}$$

C. Hybrid Non-redundant Arrays

Now, we design hybrid non-redundant arrays which not only enjoy reduced mutual coupling but also achieve the desired array aperture. This can be realized by modifying the disjunctive optimization problem (19) as follows:

$$\begin{aligned}
& \max_{p_n \in \mathbb{Z}^+, \forall n} p_N \\
& \text{subject to} \quad p_N \leq \bar{A}, \\
& \quad \mathbf{Sp} \geq (1 + L_m)\mathbf{1}_{N-1}, \\
& \quad \Omega(\mathbf{j}_A^{(l)} \mathbf{p} \neq \mathbf{j}_B^{(l)} \mathbf{p}) = \text{True}, \quad l = 1, \dots, L.
\end{aligned} \tag{38}$$

The above optimization problem is feasible if a sufficiently large value of \bar{A} is selected whose lower bound is given by Eq. (37). The optimization problem (38) tends to achieve an aperture of \bar{A} such that the mutual coupling effects are reduced by employing consecutive holes in the resulting co-array for lag positions $1, \dots, L_m$. The corresponding MILP problems can be derived by following the same procedures as those in Section IV.

VI. DOA ESTIMATION

A. Compressive sensing-based method

Eq. (5) can be exploited along with compressive sensing approach, resulting in the following constrained l_0 -norm minimization:

$$\hat{\mathbf{r}} = \arg \min_{\mathbf{r}} \|\mathbf{r}\|_0 \text{ subject to } |\mathbf{B}\mathbf{r} - \hat{\mathbf{z}}|_F^2 \leq \kappa, \tag{39}$$

where $\hat{\mathbf{z}} = \text{vec}(\hat{\mathbf{R}}_x)$, κ is the user-specific error bound, and \mathbf{B} is an $N^2 \times G$ dictionary matrix consisting of a grid of searching steering vectors corresponding to angles $\theta_1, \dots, \theta_G$ such that the g th column of \mathbf{B} can be represented by $\mathbf{a}^*(\theta_g) \otimes \mathbf{a}(\theta_g)$ and $G \gg Q$. Moreover, \mathbf{r} represents a sparse vector which selects and adds the desired steering columns from \mathbf{B} . The last entry of $\hat{\mathbf{r}}$ represents the estimate of noise power $\hat{\sigma}_n^2$, whereas the positions and values of other non-zero entries in $\hat{\mathbf{r}}$ illustrate the estimated DOAs and their corresponding signal power. The LASSO-based optimization problem corresponding to (39) takes the following form [40]:

$$\hat{\mathbf{r}} = \arg \min_{\mathbf{r}} \|\mathbf{B}\mathbf{r} - \hat{\mathbf{z}}\|_F^2 + \eta \|\mathbf{r}\|_1, \tag{40}$$

where η is the regularization parameter which controls the trade-off between the Frobenius norm minimization-based fitting and l_1 -norm based sparsity measure.

B. Array interpolation-based method

We can employ structured matrix completion to fill the holes in the difference co-array resulting from the non-redundant sparse arrays. A binary vector \mathbf{v} can be constructed to illustrate the presence of real and virtual sensors. The i -th element of \mathbf{v} is given as:

$$v_i = \begin{cases} 1, & i \in \mathbb{P}, \\ 0, & i \in \mathbb{P}', \end{cases} \tag{41}$$

where $i = 0, \dots, p_N$ and \mathbb{P}' is the compliment set of \mathbb{P} . The received signal from the non-redundant array takes the following form:

$$\mathbf{y}(t) = \mathbf{u}(t) \circ \mathbf{v}, \tag{42}$$

where $\mathbf{u}(t)$ denotes the signal received by a hypothetical ULA of aperture p_N having an inter-element spacing of $\lambda/2$.

If $\hat{\mathbf{R}}_{yy}$ is the estimated covariance matrix of $\mathbf{y}(t)$, we can represent its missing entries with a mask $\mathbf{V} = \mathbf{v}\mathbf{v}^H$ where the zeros in \mathbf{V} correspond to the missing entries in $\hat{\mathbf{R}}_{yy}$. Recall that the covariance matrix of a ULA has ideally a Hermitian Toeplitz structure. Therefore, the matrix completion problem for covariance matrix recovery can be expressed as the following semi-definite optimization problem [27]:

$$\begin{aligned}
& \min_{\mathbf{w}} \text{rank}(\mathcal{T}(\mathbf{w})) \\
& \text{subject to} \quad |\mathcal{T}(\mathbf{w}) \circ \mathbf{V} - \hat{\mathbf{R}}_{yy}|_F^2 \leq \gamma, \\
& \quad \mathcal{T}(\mathbf{w}) \succeq 0,
\end{aligned} \tag{43}$$

where $\mathcal{T}(\mathbf{w})$ represents the Toeplitz and Hermitian matrix with \mathbf{w} as the first column and γ is the error tolerance.

We can relax the rank minimization objective in (43) by exploiting the nuclear norm of $\mathcal{T}(\mathbf{w})$ given by $\|\mathcal{T}(\mathbf{w})\|_* = \text{tr}(\sqrt{\mathcal{T}^H(\mathbf{w})\mathcal{T}(\mathbf{w})})$ which can be further relaxed as $\text{tr}(\mathcal{T}(\mathbf{w}))$ [38]. The optimization problem (43) takes the following convex form:

$$\begin{aligned}
& \min_{\mathbf{w}} \|\mathcal{T}(\mathbf{w}) \circ \mathbf{B} - \hat{\mathbf{R}}_{yy}\|_F^2 + \zeta \text{tr}(\mathcal{T}(\mathbf{w})) \\
& \text{subject to} \quad \mathcal{T}(\mathbf{w}) \succeq 0,
\end{aligned} \tag{44}$$

where ζ is the regularization parameter. After the covariance matrix of the interpolated sparse array is extracted, we can

subsequently employ popular subspace-based DOA estimation methods, e.g., MUSIC [35] and ESPRIT [36], to obtain the DOA estimates.

VII. NUMERICAL EXAMPLES

In this section, we provide numerical examples to illustrate the superiority of the proposed array designs in terms of number of DOFs, weight functions, DOA estimation performance, and mutual coupling effects compared to popular array structures of coprime array [10], nested array [9], coprime array with minimum lag redundancies (CAMLR) [20], MRA [3], super nested array (SNA) [16], augmented nested array (ANA) [14], and MISC array [5]. We construct the proposed array structures of NNRA, optimized non-redundant array with minimum array aperture (ONRA, i.e., MHA), optimized non-redundant array with desired aperture (ONRA_{da}), optimized non-redundant array for reduced mutual coupling (ONRA_{mc}), and hybrid optimized non-redundant array (ONRA_{hybrid}). ONRA_{hybrid} combines the desired features of ONRA_{da} and ONRA_{mc}. We consider the desired array aperture of $p_N = 22$ for ONRA_{da} and ONRA_{hybrid}, whereas L_m is fixed to be 1 for ONRA_{mc} and ONRA_{hybrid}. The Big-M formulation of MILP optimizations has been used to extract sensor locations for all the proposed array configurations.

A. Degrees-of-freedom and Weight Functions

Fig. 1 shows all the sparse array structures under consideration. Their resulting non-zero co-array lags can be observed from their weight functions in Fig. 2. It is shown that coprime array, nested array, CAMLR, MRA, SNA, ANA, and MISC array respectively achieve 9, 12, 12, 14, 12, 13, 14 unique non-negative co-array lags. On the other hand, all the proposed array structures provide maximum number of non-negative unique lags equal to 16. We can also observe that NNRA has a very large array aperture, whereas ONRA, ONRA_{da},

ONRA_{mc}, and ONRA_{hybrid} enjoy array compactness and have the respective optimized array aperture of 17, 22, 20, and 22, respectively.

It can be observed from Fig. 2 that coprime array, nested array, CAMLR, MRA, SNA, ANA, and MISC array have a high number of small non-negative lags. This shows that DOA estimation using these arrays will be significantly affected by mutual coupling effects. On the other hand, the proposed array structures NNRA, ONRA and ONRA_{da} have only one co-array lag at the positions 1, 2, and 3. Therefore, these array structures are less susceptible to the undesired mutual coupling effects. Moreover, the non-redundant arrays ONRA_{mc} and ONRA_{hybrid}, which are specifically designed to avoid mutual coupling effects using $L_m = 1$, have holes at co-array lag 1 that further reduces the influence of mutual coupling for these array structures. From Figs. 1 and 2, we observe that ONRA_{hybrid} enjoys the desirable benefits of both ONRA_{da} and ONRA_{mc}, i.e., it achieves the desired aperture of 22 and has a hole at lag position 1. Therefore, ONRA_{hybrid} has the ability to provide high resolution DOA estimates while mitigating the undesired mutual coupling effects. Another interesting observation is that the minimum inter-element spacing for ONRA_{mc} and ONRA_{hybrid} is one wavelength. However, these arrays do not experience any angle ambiguities as the minimum co-array spacing is half-wavelength which is evident from Fig. 2.

B. DOA Estimation in the Absence of Mutual Coupling

We compare the DOA estimation performance of all the arrays under consideration for the case of six sensors and $Q = 13$ sources uniformly distributed from -48° to 48° . We use 500 snapshots of data for DOA estimation, and the input signal-to-noise ratio (SNR) is fixed at 0 dB. Mutual coupling among the sensors is ignored in this subsection.

Fig. 3 shows the LASSO spectra for the 12 sparse arrays being compared using $\eta = 2.5$ and a grid size of 0.1° . It is observed that all the design examples other than the non-redundant arrays fail to successfully resolve all sources, and inherent bias is clearly observed in these estimation results. In comparison, all non-redundant arrays are able to resolve all the sources. Note that NNRA results in some false peaks due to the high sidelobe level as the array is highly sparse. On the other hand, the proposed ONRA, ONRA_{da}, ONRA_{mc}, ONRA_{hybrid} do not produce any artifacts and achieve a clean LASSO spectrum. This fact verifies their superior DOA estimation capability.

To obtain the hole-free covariance matrix using structured matrix completion, the value of ζ is assumed to be 0.1 for all simulations. Fig. 4 shows the MUSIC and ESPRIT spectra of all the arrays under consideration while employing structured matrix completion. Normalized spectrum is plotted for MUSIC, and the DOA estimates for ESPRIT are plotted using '+' marks in the same plots. It is observed that the use of structured matrix completion significantly improves the DOA estimation capability of many array designs under consideration. For instance, almost all the conventional designs can resolve most of the sources; however, several estimates

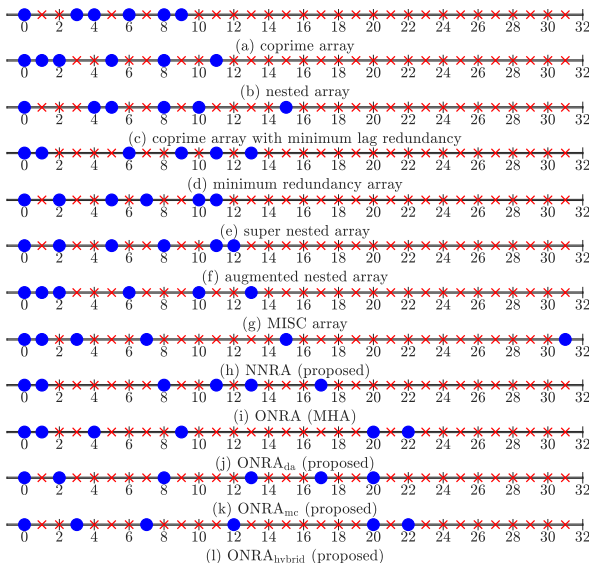


Fig. 1. Array structures of different types of 6-element sparse arrays under consideration.

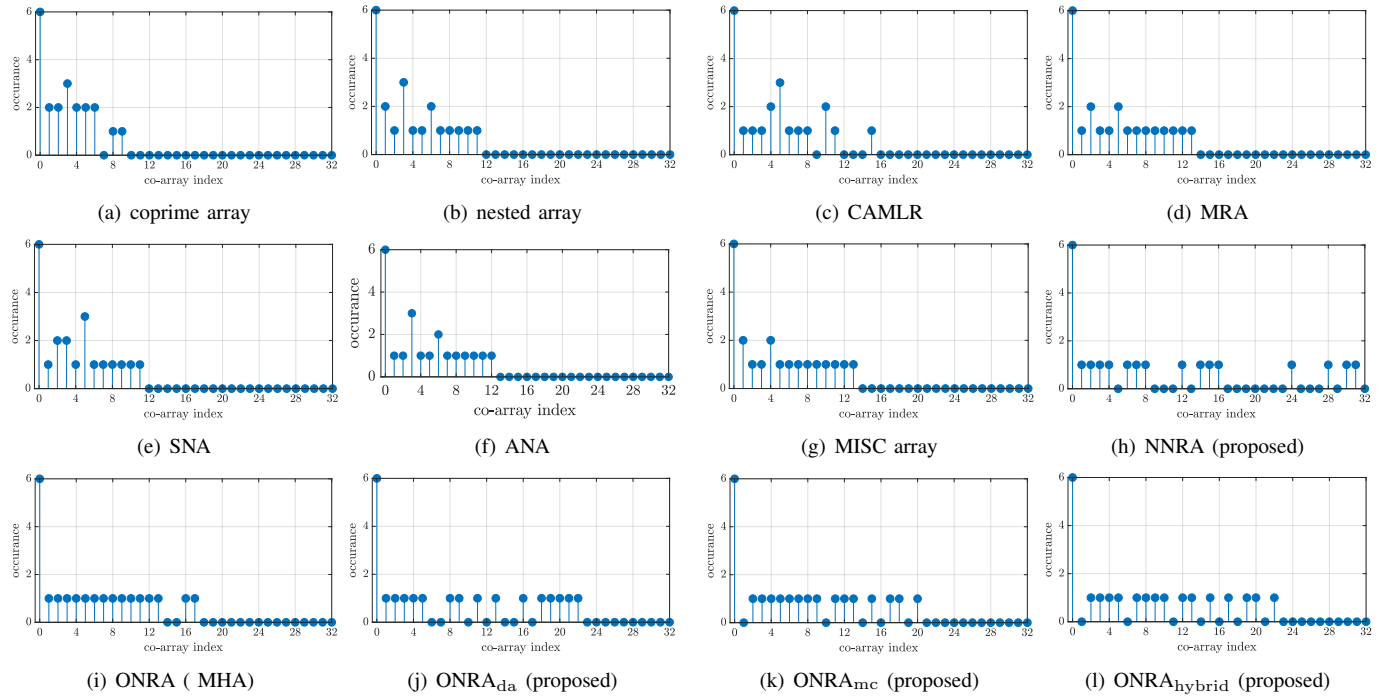


Fig. 2. The non-negative co-array weight functions of twelve different types of 6-element sparse arrays under consideration.

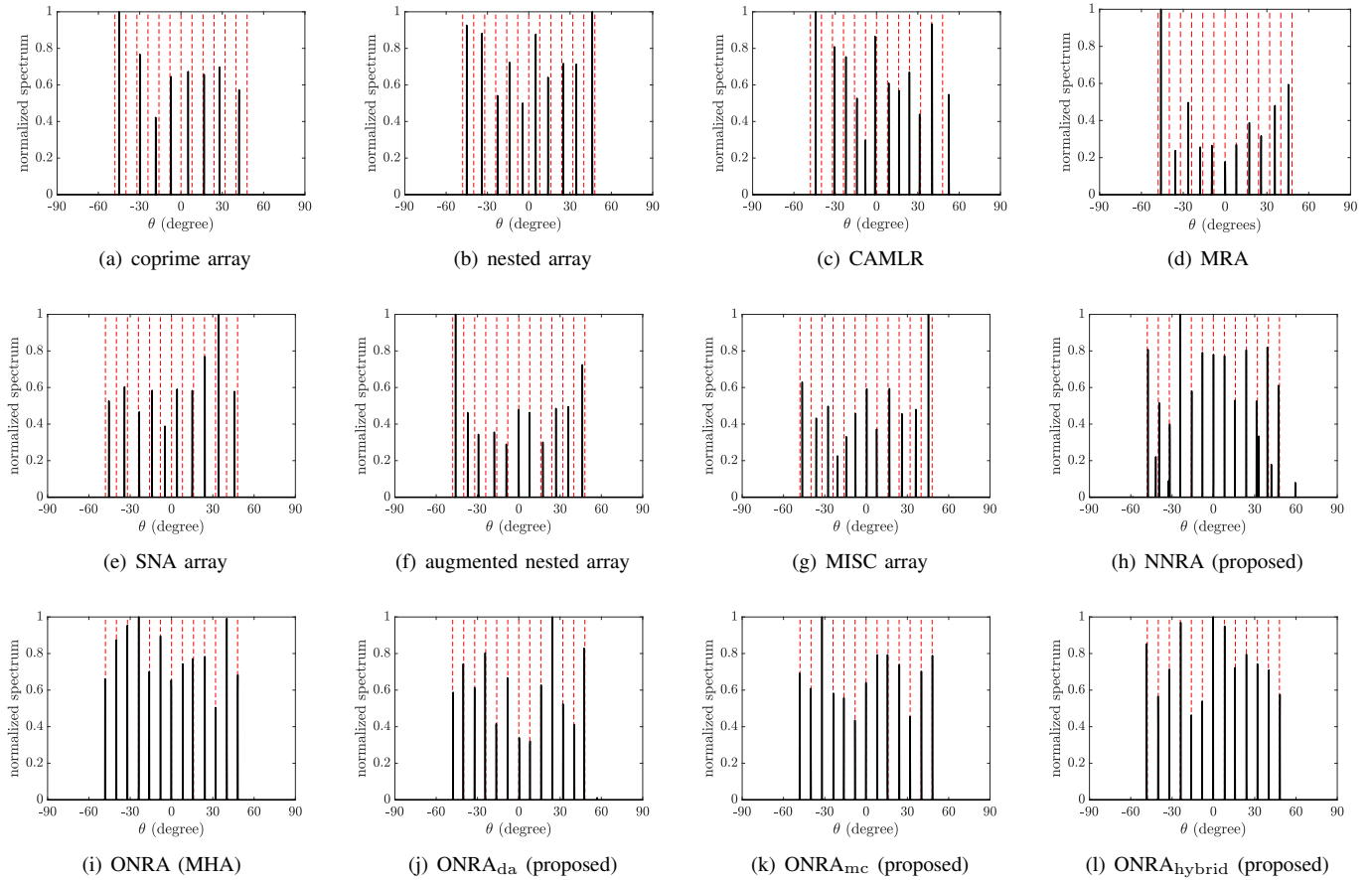


Fig. 3. The normalized LASSO spectra for twelve different types of 6-element sparse arrays. $Q = 13$ sources are uniformly distributed between -48° and 48° , SNR is 0 dB, the number of snapshots is 500, the grid size for LASSO is 0.1° , and the regularization parameter η is 2.5.

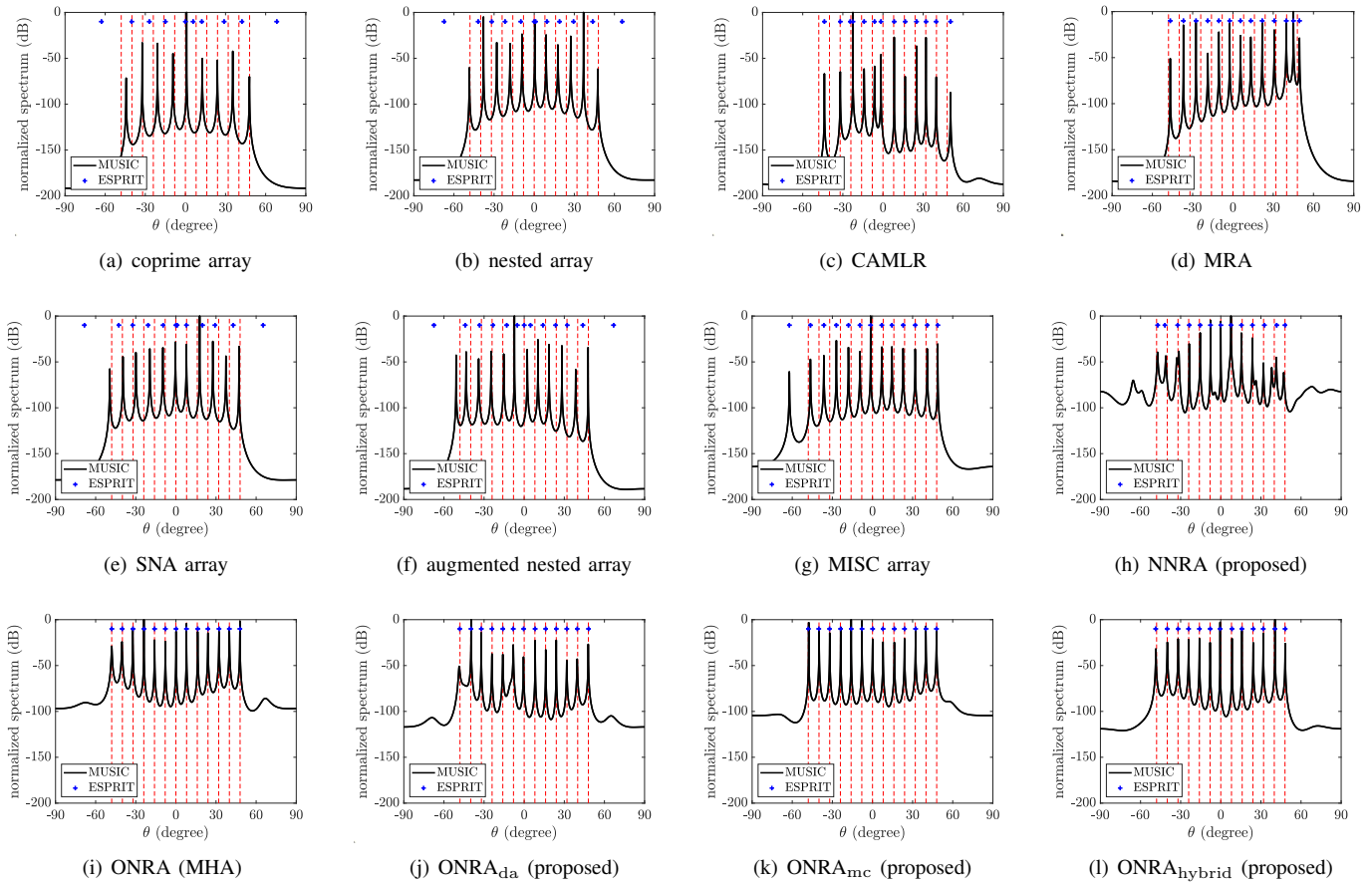


Fig. 4. The MUSIC spectra and ESPRIT results for twelve different types of 6-element sparse arrays. $Q = 13$ sources are uniformly distributed between -48° and 48° , SNR is 0 dB, the number of snapshots is 500, and $\zeta = 0.1$.

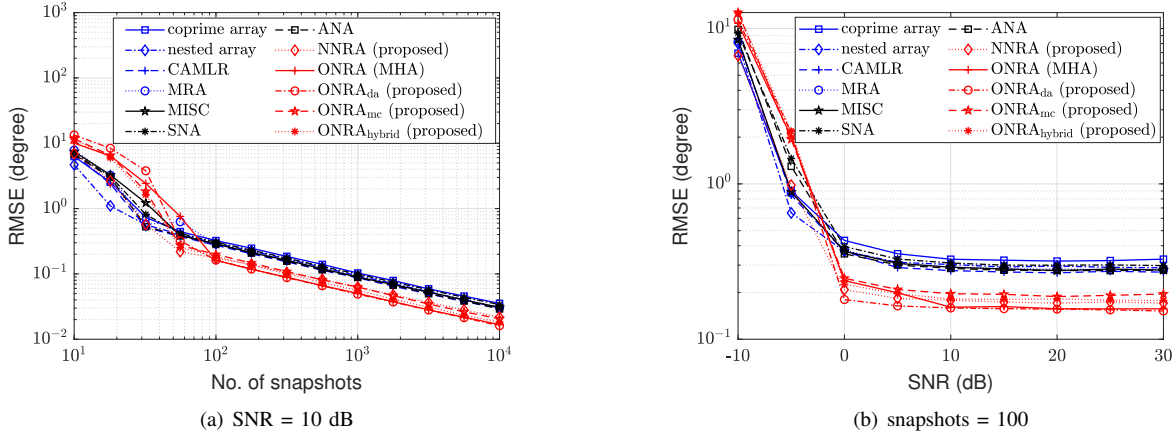


Fig. 5. RMSE of DOA estimates exploiting ESPRIT in the absence of mutual coupling when $Q = 5$ sources are located at $\theta = [-30^\circ, -15^\circ, 0^\circ, 15^\circ, 30^\circ]$ ($\zeta = 0.1$, 1000 Monte Carlo trials).

are biased. NNRA resolves all sources with a lower bias, but it contains false peaks because of its highly sparse array design which yields high sidelobe levels. This result confirms the importance of having certain cardinality with consecutive lags for effective matrix completion [24]. On the other hand, ONRA, ONRA_{da}, ONRA_{mc}, and ONRA_{hybrid} achieve accurate DOA estimation performance by providing unbiased high-resolution DOA estimates, thereby demonstrating their superior performance.

Now we investigate the root mean squared error (RMSE)

performance of the sparse arrays under consideration. For these simulations, we consider 5 independent sources impinging on the arrays under consideration at angles -30° , -15° , 0° , 15° , and 15° , respectively. For all the array designs, we apply structured matrix completion-based co-array interpolation and subsequently exploit ESPRIT algorithm to extract DOA estimates. Fig. 5(a) shows that all the proposed array designs provide low RMSE for a varying number of snapshots compared to the other array structures. A similar trend is observed in Fig. 5(b) where the RMSE performance

is compared with varying input SNR. We observe that the RMSE performance of all the proposed non-redundant array structures is very close to each other. However, it is observed that the proposed array designs have worse DOA estimation performance when the number of snapshots is small or when the input SNR is low. In such cases, the higher redundancy offered in other array designs can contribute to compensate the effect of noise and covariance matrix perturbation, whereas the proposed non-redundant array designs lack such capability. Such performance degradation is common in sparse signal processing whose superiority is more clear in scenarios with a high SNR and a large number of snapshots. We maintain, however, that there are many real-world applications, such as radar and sonar after coherent range and Doppler processing, that would offer an adequate level of SNR and a large number of snapshots to benefit from the proposed non-redundant array designs.

In order to investigate the capability of the proposed array designs to resolve closely spaced sources, we consider two sources located at $\theta_1 = 20^\circ$ and $\theta_2 = 23^\circ$, respectively. The input SNR is fixed at 0 dB, whereas the number of snapshots is reduced to 50. The histogram of 5000 Monte Carlo trials is plotted in Fig. 6(a). DOA estimates exploiting NNRA, ONRA (MHA), ONRA_{da}, ONRA_{mc}, and ONRA_{hybrid} yields an RMSE of 0.0664, 1.7794, 0.2873, 0.7738, 0.2867, respectively. It is observed that, due to the large array aperture, NNRA gives the best resolution for closely spaced sources. On the other hand, ONRA (MHA) gives the worst performance. Best performance is demonstrated by ONRA_{da} and ONRA_{hybrid} because both array structures enjoy the same large array aperture. ONRA (MHA) and ONRA_{mc} show worse performance because they were not able to resolve the two closely-spaced sources successfully in all the trials due to their smaller array aperture. This result illustrates the importance of flexibility in the array aperture provided by proposed generalized non-

redundant array designs.

C. DOA Estimation in the Presence of Mutual Coupling

Now, we investigate the DOA performance of arrays under consideration for the case of very high mutual coupling. For this purpose, we consider $|c_k| = |c_1|/k$, for $k = 2, \dots, C$, $|c_1| = 0.3$ and $C = 100$. Fig. 6(b) shows the histogram of DOA estimates in the range of $[19^\circ, 24^\circ]$ for 5000 independent trials. DOA estimates exploiting NNRA, ONRA (MHA), ONRA_{da}, ONRA_{mc}, and ONRA_{hybrid} have an RMSE of 0.0979, 7.8773, 2.1930, 1.5832, 0.5150, respectively. We see that the ONRA (MHA) has a significantly higher failure rate to resolve the two sources within the range $[19^\circ, 24^\circ]$ in the presence of mutual coupling. ONRA_{da} also has poor DOA estimation performance due to the presence of a lag at location 1. On the other hand, ONRA_{mc}, which is specifically designed to reduce mutual coupling effects, performs better than ONRA (MHA) and ONRA_{da}. Moreover, NNRA and ONRA_{hybrid} provide the best performance due to their large inter-element spacings compared to other arrays. The RMSE results for this case exploiting ESPRIT with varying influence of mutual coupling are plotted in Fig. 7(a). It is observed that the NNRA performs better when the mutual coupling effect is low. However, note that the success of NNRA is also partially due to the large array aperture, leading to a high DOA resolution. When the mutual coupling effects become high, the performance of NNRA degrades rapidly. Among the optimized array designs, ONRA_{hybrid} and ONRA_{mc} outperform all other non-redundant designs and the existing sparse array structures under consideration. When the number of sources is increased, Fig. 7(b) shows the RMSE with respect to varying mutual coupling influence. It is observed that the optimized non-redundant arrays specifically designed to mitigate the mutual coupling effects outperform all other array structures under consideration, with the ONRA_{hybrid} providing the best performance. The RMSE performance for this case with varying number of snapshots is shown in Fig. 8(a). We observe that the proposed array designs provide low RMSE for a varying number of snapshots compared to the other array structures. A similar trend is observed in Fig. 8(b) where the RMSE performance is compared with varying input SNR. We observe that the RMSE performance of hybrid array structure is the best compared to all the other array designs under consideration.

All the simulation results clearly illustrate the superiority of the proposed array design strategies.

VIII. CONCLUSIONS

In this paper, we proposed a generalized design framework for non-redundant sparse arrays that achieve highest number of DOFs for DOA estimation by providing the maximum number of co-array lags. The proposed array design strategies render difference co-arrays with no lag redundancies. The zero-redundancy design rule developed in this paper serves as a baseline for non-redundant sparse array design, and the NNRA structure is developed in a straightforward manner. We then developed a systematized array design framework based

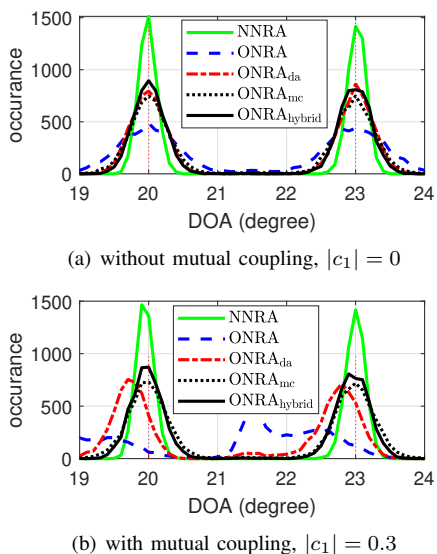


Fig. 6. Histogram of DOA estimates exploiting ESPRIT from 5,000 Monte Carlo trials. Two sources are located at $[20^\circ, 23^\circ]$ with 0 dB SNR, and 100 snapshots are considered.

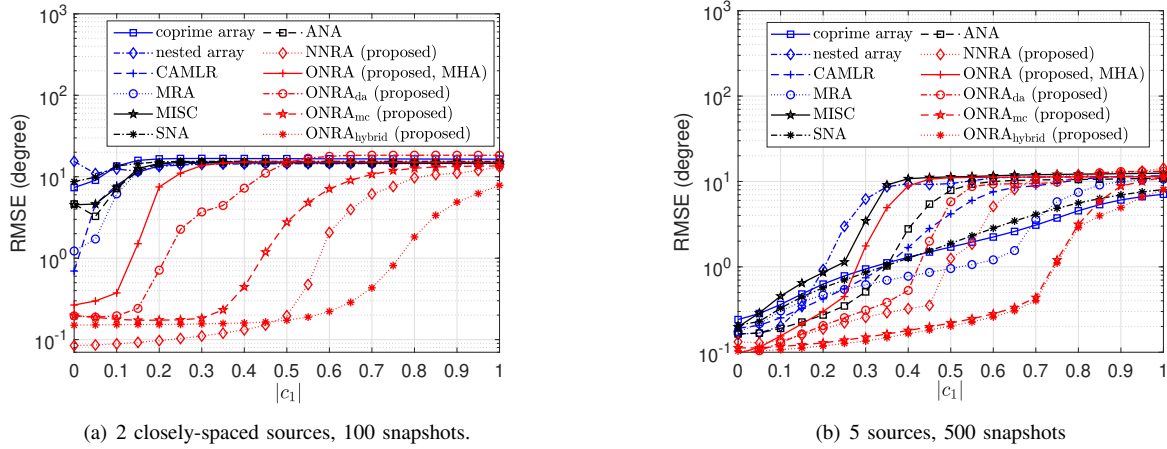


Fig. 7. RMSE of DOA estimates exploiting ESPRIT with respect to the varying magnitude of mutual coupling co-efficient c_1 (SNR = 0 dB, $|c_k| = |c_1|/k$ for $k = 2, \dots, C$, $C = 100, 500$ Monte Carlo trials): (a) $\theta = [20^\circ, 23^\circ]$, (b) $\theta = [-30^\circ, -15^\circ, 0^\circ, 15^\circ, 30^\circ]$.

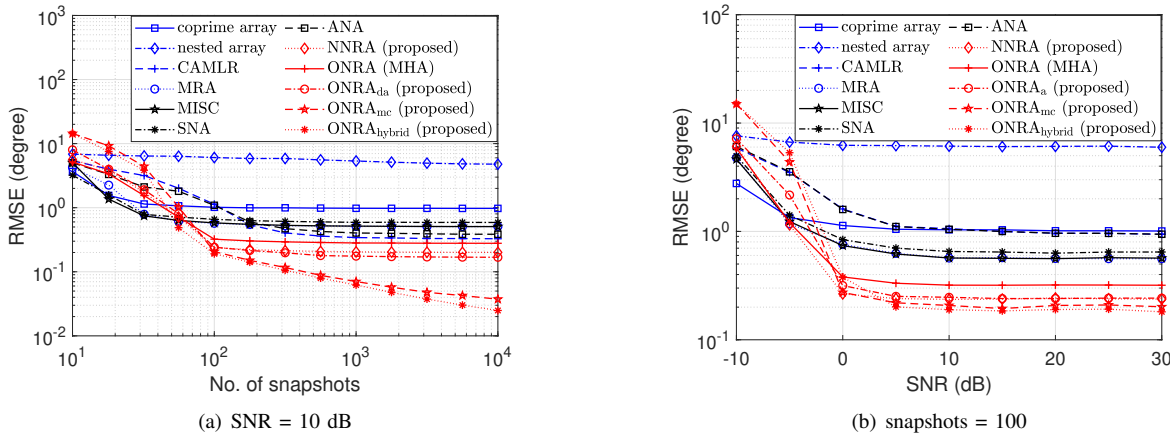


Fig. 8. RMSE of DOA estimates exploiting ESPRIT in the presence of mutual coupling when $Q = 5$ sources are located at $\theta = [-30^\circ, -15^\circ, 0^\circ, 15^\circ, 30^\circ]$ ($\zeta = 0.1$, $|c_k| = |c_1|/k$ for $k = 2, \dots, C$, $C = 100, 1000$ Monte Carlo trials).

on disjunctive programming, and the results are expanded to two MILP optimization problems which can be solved using popular solvers. In addition to developing non-redundant arrays with a minimum array aperture, we generalize the non-redundant sparse array design framework with desired features that use flexible array apertures and reduce the mutual coupling effects. Employing structured matrix completion interpolates missing holes in the resultant co-array and enables gridless DOA estimation. Simulation results were performed by exploiting LASSO-based strategy on the resulting difference co-array as well as MUSIC and ESPRIT using the interpolated co-array. The hybrid non-redundant array structure enjoys both desired array aperture and mutual coupling reduction capability and provides best overall performance.

REFERENCES

- [1] T. E. Tuncer and B. Friedlander (Eds.), *Classical and Modern Direction-of-Arrival Estimation*. Elsevier, 2009.
- [2] R. T. Hoctor and S. A. Kassam, "The unifying role of the co-array in aperture synthesis for coherent and incoherent imaging," *Proc. IEEE*, vol. 78, no. 4, pp. 735–752, April 1990.
- [3] A. Moffet, "Minimum-redundancy linear arrays," *IEEE Trans. Antennas Propagat.*, vol. 16, no. 2, pp. 172–175, March 1968.
- [4] C. L. Liu and P. P. Vaidyanathan, "Hourglass arrays and other novel 2-D sparse arrays with reduced mutual coupling," *IEEE Trans. Signal Process.*, vol. 65, no. 13, pp. 3369–3383, July 2017.
- [5] Z. Zheng, W. Wang, Y. Kong and Y. D. Zhang, "MISC Array: A new sparse array design achieving increased degrees of freedom and reduced mutual coupling effect," *IEEE Trans. Signal Process.*, vol. 67, no. 7, pp. 1728–1741, April 2019.
- [6] S. Pillai and F. Haber, "Statistical analysis of a high resolution spatial spectrum estimator utilizing an augmented covariance matrix," *IEEE Trans. Acoust., Speech, Signal Process.*, vol. 35, no. 11, pp. 1517–1523, Nov. 1987.
- [7] E. Vertatschitsch and S. Haykin, "Nonredundant arrays," *Proc. IEEE*, vol. 74, no. 1, pp. 217–217, Jan. 1986.
- [8] D. A. Linebarger, I. H. Sudborough, and I. G. Tollis, "Difference bases and sparse sensor arrays," *IEEE Trans. Inf. Theory*, vol. 39, no. 2, pp. 716–721, Mar. 1993.
- [9] P. Pal and P. P. Vaidyanathan, "Nested arrays: A novel approach to array processing with enhanced degrees of freedom," *IEEE Trans. Signal Process.*, vol. 58, no. 8, pp. 4167–4181, Aug. 2010.
- [10] P. P. Vaidyanathan and P. Pal, "Sparse sensing with co-prime samplers and arrays," *IEEE Trans. Signal Process.*, vol. 59, no. 2, pp. 573–586, Feb. 2011.

- [11] P. Pal and P. P. Vaidyanathan, "Multiple level nested array: An efficient geometry for 2qth order cumulant based array processing," *IEEE Trans. Signal Process.*, vol. 60, no. 3, pp. 1253–1269, Mar. 2012.
- [12] P. Pal and P. P. Vaidyanathan, "Nested arrays in two dimensions, Part I: Geometrical considerations," *IEEE Trans. Signal Process.*, vol. 60, no. 9, pp. 4694–4705, Sep. 2012.
- [13] P. Pal and P. P. Vaidyanathan, "Nested arrays in two dimensions, Part II: Application in two dimensional array processing," *IEEE Trans. Signal Process.*, vol. 60, no. 9, pp. 4706–4718, Sep. 2012.
- [14] J. Liu, Y. Zhang, Y. Lu, S. Ren, and S. Cao, "Augmented nested arrays with enhanced DOF and reduced mutual coupling," *IEEE Trans. Signal Process.*, vol. 65, no. 21, pp. 5549–5563, Nov. 2017.
- [15] S. Qin, Y. D. Zhang, and M. G. Amin, "Generalized coprime array configurations for direction-of-arrival estimation," *IEEE Trans. Signal Process.*, vol. 63, no. 6, pp. 1377–1390, March 2015.
- [16] C. L. Liu and P. P. Vaidyanathan, "Super nested arrays: Linear sparse arrays with reduced mutual coupling—Part I: Fundamentals," *IEEE Trans. Signal Process.*, vol. 64, no. 15, pp. 3997–4012, Aug. 2016.
- [17] C. L. Liu and P. P. Vaidyanathan, "Super nested arrays: Linear sparse arrays with reduced mutual coupling—Part II: High-order extensions," *IEEE Trans. Signal Process.*, vol. 64, no. 16, pp. 4203–4217, Aug. 2016.
- [18] D. Bush and N. Xiang, "n-tuple coprime sensor arrays," *J. Acoust. Soc. Am.*, vol. 142, no. EL567, 2017.
- [19] S. A. Alawsh and A. H. Muqaibel, "Multi-level prime array for sparse sampling," *IET Signal Process.*, vol. 12, no. 6, pp. 688–699, Aug. 2018.
- [20] A. Ahmed, Y. D. Zhang and J.-K. Zhang, "Coprime array design with minimum lag redundancy," in *Proc. IEEE Int. Conf. Acoustics, Speech, Signal Process.*, Brighton, UK, May 2019, pp. 4125–4129.
- [21] Z. Shi, C. Zhou, Y. Gu, N. A. Goodman, and F. Qu, "Source estimation using coprime array: A sparse reconstruction perspective," *IEEE Sensors J.*, vol. 17, no. 3, pp. 755–765, Feb. 2017.
- [22] C. Zhou, Y. Gu, Y. D. Zhang, Z. Shi, T. Jin, and X. Wu, "Compressive sensing-based coprime array direction-of-arrival estimation," *IET Commun.*, vol. 11, no. 11, pp. 1719–1724, Aug. 2017.
- [23] Y. D. Zhang, M. G. Amin, and B. Himed, "Sparsity-based DOA estimation using co-prime arrays," in *Proc. IEEE Int. Conf. Acoust., Speech, Signal Process.*, Vancouver, Canada, May 2013, pp. 3967–3971.
- [24] H. Qiao and P. Pal, "Unified analysis of co-array interpolation for direction-of-arrival estimation," in *Proc. IEEE Int. Conf. on Acoustics, Speech, Signal Process.*, New Orleans, LA, March 2017, pp. 3056–3060.
- [25] H. Qiao and P. Pal, "Gridless line spectrum estimation and low rank Toeplitz matrix compression using structured samplers: A regularization-free approach," *IEEE Trans. Signal Process.*, vol. 65, no. 9, pp. 2221–2236, May 2017.
- [26] X. Wu, W.-P. Zhu, and J. Yan, "A Toeplitz covariance matrix reconstruction approach for direction-of-arrival estimation," *IEEE Trans. Veh. Technol.*, vol. 66, no. 9, pp. 8223–8237, Sep. 2017.
- [27] C. Zhou, Y. Gu, X. Fan, Z. Shi, G. Mao, and Y. D. Zhang, "Direction-of-arrival estimation for coprime array via virtual array interpolation," *IEEE Trans. Signal Process.*, vol. 66, no. 22, pp. 5956–5971, Nov. 2018.
- [28] E. Balas, *Disjunctive Programming*. Springer, 2018.
- [29] I. E. Grossmann and , "Generalized disjunctive programming: A framework for formulation and alternative algorithms for MINLP optimization," in *Mixed Integer Nonlinear Programming*, vol. 154. Springer, 2012.
- [30] GAMS Development Corporation, "General algebraic modeling system (GAMS) release 27.1.0," Fairfax, VA, USA, 2019.
- [31] W. E. Hart, C. D. Laird, J.-P. Watson, D. L. Woodruff, G. A. Hackebeil, B. L. Nicholson, and J. D. Sirola, *Pyomo – Optimization Modeling in Python*, 2nd Ed., Springer, 2017.
- [32] Gurobi, "Gurobi optimizer reference manual," <http://www.gurobi.com>
- [33] MosekApS, "The MOSEK optimization toolbox for MATLAB manual. Version 9.0.," 2019. <http://docs.mosek.com/9.0/toolbox/index.html>
- [34] A. Ahmed and Y. D. Zhang, "Non-redundant sparse array with flexible aperture," in *Proc. Asilomar Conf. Signals, Syst. Comput.*, Pacific Grove, CA, Nov. 2020.
- [35] R. Schmidt, "Multiple emitter location and signal parameter estimation," *IEEE Trans. Antennas Propag.*, vol. 34, no. 3, pp. 276–280, March 1986.
- [36] R. Roy and T. Kailath, "ESPRIT—estimation of signal parameters via rotational invariance techniques," *IEEE Trans. Acoust., Speech, Signal Process.*, vol. 37, no. 7, pp. 984–995, July 1989.
- [37] S. Golomb, "How to number a graph," in *Graph Theory and Computing*, R. Reed, Ed. Academic Press, 1972, pp. 23–37.
- [38] E. J. Candès, B. Recht, "Exact matrix completion via convex optimization," *Found. Comput. Math.*, vol. 9, pp. 717–772, April 2009.
- [39] CVX Research, Inc. "CVX: Matlab software for disciplined convex programming," version 2.0. <http://cvxr.com/cvx>, April 2011.
- [40] R. Tibshirani, "Regression shrinkage and selection via the lasso," *J. Royal Stat. Soc., Ser. B*, vol. 58, no. 1, pp. 267–288, 1996.



Ammar Ahmed (S'17) received Ph.D. degree in electrical engineering from Temple University, Philadelphia, USA, in 2021. Currently, he is working as a radar signal processing engineer at Aptiv, Agoura Hills, CA, USA. His research interests are in digital signal processing, optimization, and radar systems.



Yimin D. Zhang (F'19) received the Ph.D. degree from the University of Tsukuba, Tsukuba, Japan, in 1988.

He is currently an Associate Professor with the Department of Electrical and Computer Engineering, Temple University, Philadelphia, PA, USA. From 1998 to 2015, he was a Research Faculty with the Center for Advanced Communications, Villanova University, Villanova, PA, USA. His research interests include array signal processing, compressive sensing, machine learning, convex optimization, and

time-frequency analysis with applications to radar, wireless communications, and satellite navigation.

Dr. Zhang is an Associate Editor for *IEEE Transactions on Aerospace and Electronic Systems* and for *Signal Processing*. He was an Associate Editor for *IEEE Transactions on Signal Processing*, *IEEE Signal Processing Letters*, and *Journal of the Franklin Institute*. He was a Technical Co-Chair of the 2018 IEEE Sensor Array and Multichannel Signal Processing Workshop. He was the recipient of the 2016 IET Radar, Sonar & Navigation Premium Award, the 2017 IEEE AESS Harry Rowe Mimmo Award, the 2019 IET Communications Premium Award, and the 2021 EURASIP Best Paper Award for Signal Processing. He coauthored a paper that received the 2018 IEEE Signal Processing Society Young Author Best Paper Award. He is a fellow of SPIE.